Molecular Therapy
Nucleic Acids
Original Article

STAT3 Gene Silencing by Aptamer-siRNA Chimera as Selective Therapeutic for Glioblastoma

Carla Lucia Esposito,[1] Silvia Nuzzo,[1,2] Silvia Catuogno,[1] Simona Romano,[2] Filomena de Nigris,[3,4] and Vittorio de Franciscis[1]

[1]IEOS, CNR, Naples, Italy; [2]Department of Molecular Medicine and Medical Biotechnology, "Federico II" University of Naples, Naples, Italy; [3]Department of Biochemistry, Biophysics and General Pathology, University of Campania "Luigi Vanvitelli," Naples, Italy; [4]Sbarro Institute for Cancer Research and Molecular Medicine, Center for Biotechnology, College of Science and Technology, Temple University, Philadelphia, PA, USA

Glioblastoma (GBM) is the most frequent and aggressive primary brain tumor in adults, and despite advances in neuro-oncology, the prognosis for patients remains dismal. The signal transducer and activator of transcription-3 (STAT3) has been reported as a key regulator of the highly aggressive mesenchymal GBM subtype, and its direct silencing (by RNAi oligonucleotides) has revealed a great potential as an anti-cancer therapy. However, clinical use of oligonucleotide-based therapies is dependent on safer ways for tissue-specific targeting and increased membrane penetration. The objective of this study is to explore the use of nucleic acid aptamers as carriers to specifically drive a STAT3 siRNA to GBM cells in a receptor-dependent manner. Using an aptamer that binds to and antagonizes the oncogenic receptor tyrosine kinase PDGFRβ (Gint4.T), here we describe the design of a novel aptamer-siRNA chimera (Gint4.T-STAT3) to target STAT3. We demonstrate the efficient delivery and silencing of STAT3 in PDGFRβ$^+$ GBM cells. Importantly, the conjugate reduces cell viability and migration *in vitro* and inhibits tumor growth and angiogenesis *in vivo* in a subcutaneous *xenograft* mouse model. Our data reveals Gint4.T-STAT3 conjugate as a novel molecule with great translational potential for GBM therapy.

INTRODUCTION

Glioblastoma (GBM) is the most frequent and aggressive primary brain tumor in adults, classified as grade IV by the World Health Organization.[1,2] Treatments for GBM patients consist of tumor resection, radiotherapy, and chemotherapy. However, despite advances in surgical and medical neuro-oncology, the prognosis for GBM patients remains dismal.

A number of transcription factors and micro-RNAs governing tumor cell spreading, proliferation, and immune-surveillance escape appear to play a critical role in maintaining the malignant phenotype characterized by the deregulation of different signaling pathways, such as phosphoinositide-3 kinase, AKT, mitogen-activated protein kinases (MAPK), and the Rho family of GTPases.[3–5] Among other factors, expression and activation of the signal transducer and activator of transcription-3 (STAT3) has been reported as a key regulator of the highly aggressive mesenchymal GBM subtype[6–8] and of survival and propagation of glioma stem-like cells (GSCs).[9,10]

In response to signaling initiated by specific interleukins and growth factor receptors, including the interleukin-6 (IL-6) and the epidermal growth factor (EGF) receptors, STAT3 becomes phosphorylated and translocates into the nuclei, where it regulates the expression of genes involved in the cell cycle, survival, hypoxia, angiogenesis, invasion, and immune response.[11–13] Indeed, the deregulation of STAT3 expression and activation has been implicated not only in GBM but also in other cancer types, including leukemias and colon, renal, and breast cancers.[14,15]

Several promising STAT3 antagonists have been recently developed, including short interfering RNAs (siRNAs), antisense oligonucleotides (ASO), and decoy DNAs, as well as small molecules and peptides that act either as direct inhibitors of STAT3 phosphorylation and dimerization or indirect regulators of Janus or receptor kinases.[16] However, despite STAT3's potential as a therapeutic target, to date none of the STAT3 inhibitors have been approved for clinical use.[17] DNA and RNA oligonucleotides directed against STAT3 offer exquisite specificity and potency, but their poor cell membrane penetrance and the lack of effective tissue-targeting selective carriers remain major weaknesses that limit their use in the majority of solid tumors.[18,19] Moreover, the presence of the tight cerebrovascular endothelium, which constitutes a physical barrier to therapeutic macromolecules, makes targeting of intracranial tumors highly challenging.[20]

Aptamers are short, single-stranded oligonucleotides that assume three-dimensional shapes to bind a given target molecule.[21] Generated through an evolutionary combinatorial process named SELEX (systematic evolution of ligands by exponential enrichment),[22] they provide high-affinity ligands and potential antagonists of disease-associated proteins. In recent years, aptamers have been identified

Received 22 October 2017; accepted 28 December 2017;
https://doi.org/10.1016/j.omtn.2017.12.021.

Correspondence: Carla Lucia Esposito, IEOS, CNR, Via T. de Amicis, 80131 Naples, Italy.
E-mail: c.esposito@ieos.cnr.it

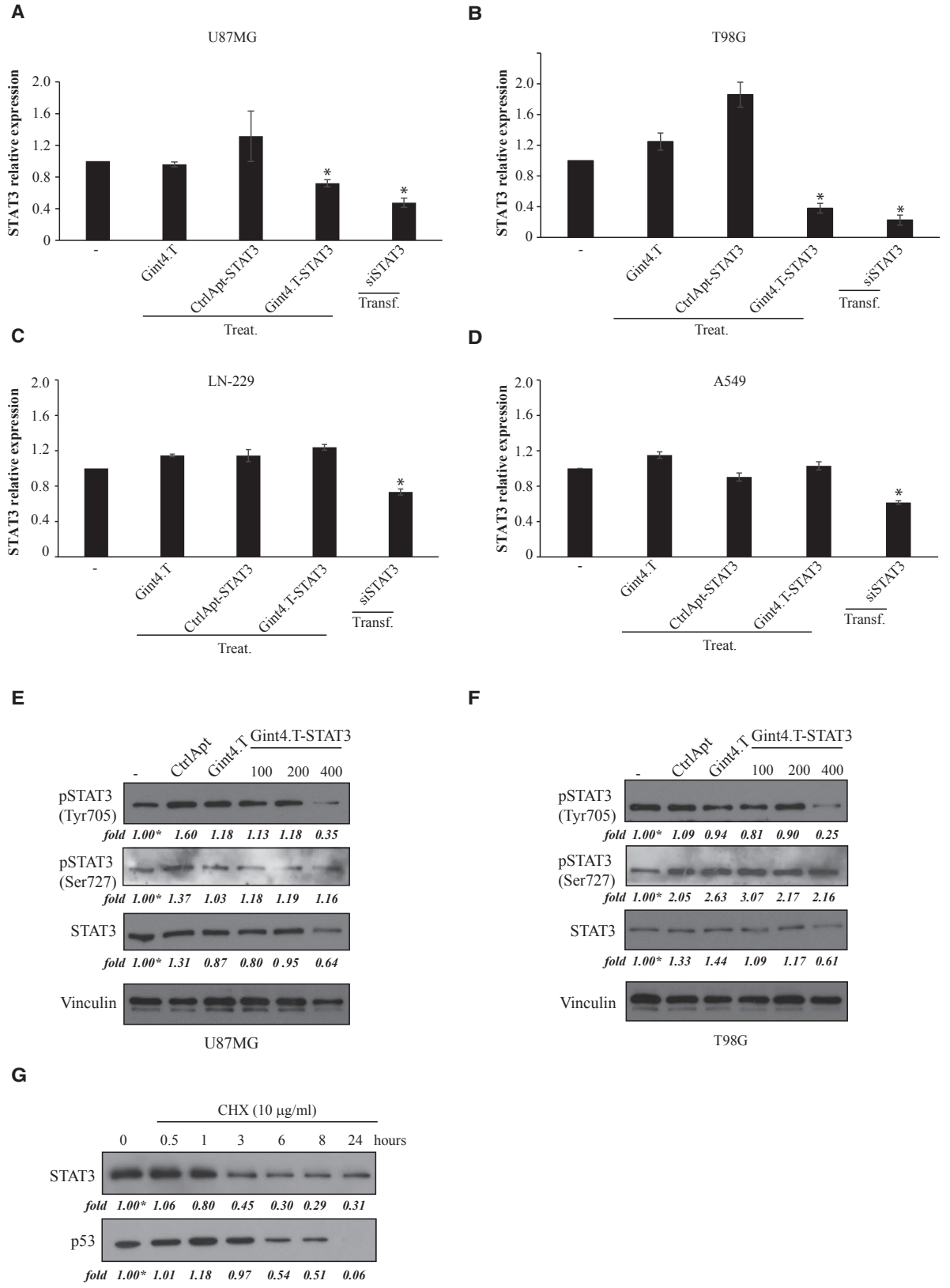

(legend on next page)

as highly promising agents for the selective delivery of secondary reagents, including therapeutic siRNAs or microRNA, nanoparticles, chemotherapeutic cargos, or molecular imaging probes, demonstrating a broad applicability both *in vitro* and *in vivo*.[23–29] Recently, aptamer-mediated STAT3 siRNA delivery has been applied to human T cell lymphomas and B cell lymphoma therapy with promising results.[30,31] In previous studies, we reported the generation of 2′-F-Pyrimidines (2′F-Py) nuclease-resistant RNA 33-mer aptamer, the Gint4.T, which binds and antagonizes the activity of the platelet-derived growth factor receptor β (PDGFRβ).[32] Further, we have recently shown that Gint4.T is able to cross a tri-culture *in vitro* model of hematoencephalic barrier, and that can act as targeting carrier to drive in a PDGFRβ-dependent manner therapeutic miRNA-based molecules to GBM cancer stem-like cells. Treatments with the aptamer-miRNA chimera results in the functional uptake of the miRNA and therapeutic target inhibition.[33] Therefore, in order to antagonize STAT3 in GBM cells, here we took advantage of Gint4.T for the design of a novel therapeutic aptamer-siRNA chimera (AsiC). We demonstrate the efficient delivery and silencing of STAT3 AsiC *in vitro* and *in vivo* in PDGFRβ-expressing GBM cell lines. We found that the conjugate combines the inhibitory action of the aptamer on PDGFRβ activity with silencing of STAT3, inducing a pronounced inhibition of cancer cell survival and migration. Most importantly, it effectively inhibited tumor growth in a *xenograft* model of GBM, thus representing a promising tool for GBM management.

RESULTS

Functional Delivery of STAT3-siRNA

By using the Gint4.T aptamer, we developed a PDGFRβ AsiC for the delivery of a previously characterized STAT3-specific siRNA antagonist.[30] To this end, we adopted the stick-based approach[33–36] for the design of the two-component conjugate (Figure S1A) and demonstrated that in the context of the chimera, the binding ability of Gint4.T (Figure S1B) as well as the STAT3 silencing function mediated by the siRNA (Figure S1C) are preserved. We thus assessed whether the Gint4.T aptamer may act as delivery moiety for the conjugated siRNA to GBM-derived cell lines. To this end, we used two GBM cell lines (U87MG and T98G) that both are positive for PDGFRβ expression and show comparable STAT3 protein levels and susceptibility to STAT3 silencing (Figures S2A and S2B). Both cell lines show a good uptake of the conjugate that reach about 64% and 73% of internalization following 1 hr of incubation in U87MG and T98G, respectively (Figures S2C and S2D). To assess AsiC-mediated STAT3 silencing, cells were treated for 72 hr with Gint4.T-STAT3 AsiC, and the levels of STAT3 mRNA were determined by qRT-PCR. As compared to treatment with Gint4.T aptamer, treating cells with the STAT3 AsiC at 400 nmol/L resulted in a significant decrease of STAT3 mRNA levels in both cell lines (to approximately 60% in U87MG and 40% in T98G) at comparable levels found upon transfection with the STAT3 siRNA moiety (Figures 1A and 1B).

To confirm that inhibition was mediated by the aptamer-dependent recognition of the PDGFRβ, we analyzed STAT3 mRNA levels upon Gint4.T-STAT3 treatment in the LN-229 GBM cell line and in the A549 non-small-cell lung cancer (NSCLC) cells that both express low levels of PDGFRβ (Figure S2A). As shown (Figures 1C and 1D), AsiC treatment did not change STAT3 mRNA levels that were instead reduced upon transfection of the siRNA moiety in both cell lines. This result indicates that AsiC-mediated STAT3 silencing is receptor-dependent both in GBM and NSCLC-derived cells.

Then, STAT3 protein levels were analyzed in U87MG and T98G (PDGFRβ$^+$) cells and we found a reduction of approximately 40% at 400 nmol/L treatment. Furthermore, since phosphorylation in Tyr 705 is required for STAT3 translocation to nucleus and gene transactivation,[37,38] we also determined the effects of AsiC treatment on pY(705)-STAT3. As shown, the pY(705)-STAT3 protein levels were strongly decreased (by approximately 70%–80% at 400 nmol/L treatment) (Figures 1E and 1F). In contrast, the levels of STAT3 proteins phosphorylated on Ser-727 (pS(727)-STAT3) remain more stable (Figures 1E and 1F). We also determined the half-life of total STAT3 protein in T98G cells in the presence of the protein synthesis inhibitor, cycloheximide (CHX). As shown, the STAT3 protein levels decrease with time for up to 6 hr, then remained stable until 24 hr, with an apparent half-life of 3 hr (Figure 1G), indicating the presence in this cell line of protein pools with different stabilities with a more stable pool of approximately 30% of total STAT3.

Together, these experiments show that the AsiC effectively delivers *in vitro* functional STAT3 siRNA into GBM target cells, downregulating STAT3.

Gint4.T-STAT3 AsiC Acts as a Cell-Selective Inhibitor of Survival and Motility

STAT3 acts as a key oncogenic factor regulating different cellular functions, including survival, proliferation, migration, and invasion.[11,39] We thus determined whether the AsiC was able to reduce cell viability *in vitro*. As assessed by MTT assay, treatment of PDGFRβ-expressing T98G and U87MG cells with 400 nmol/L

Figure 1. Gint4.T-Mediated Delivery of STAT3 siRNA

(A–D) U87MG (PDGFRβ$^+$, A),T98G (PDGFRβ$^+$, B), LN-229 (C), or A549 cells (PDGFRβ$^-$, D) cells were transfected with 100 nmol/L siSTAT3 moiety or treated with 400 nmol/L Gint4.T, Gint4.T-STAT3, control aptamer (CtrlApt), or control chimera (CtrlApt-STAT3). After 72 hr, STAT3 mRNA was quantified by qRT-PCR. Error bars depict mean ± SD. Treat, treatment; Transf., transfection. Statistics were calculated using Student's t test, *$p < 0.05$ (versus untreated). (E and F) Cell lysates from U87MG (E) or T98G (F) cells treated for 96 hr with 400 nmol/L Gint4.T or CtrlApt or with indicated concentration of Gint4.T-STAT3 AsiC were analyzed by immunoblotting with anti-pY(705)-STAT3, anti-pS(705)-STAT3, anti-STAT3, and anti-vinculin (used as a loading control) antibodies. Values below the blots indicate quantization relative to untreated (–, labeled with asterisk) normalized on the loading control signals. (G) T98G cells were left untreated or treated with CHX (10 μg/mL) for the indicated times, and cell lysates were immunoblotted with anti-STAT3 and anti-p53 (used as a positive control) antibodies. Quantization relative to untreated (labeled with asterisk) are indicated below the blots.

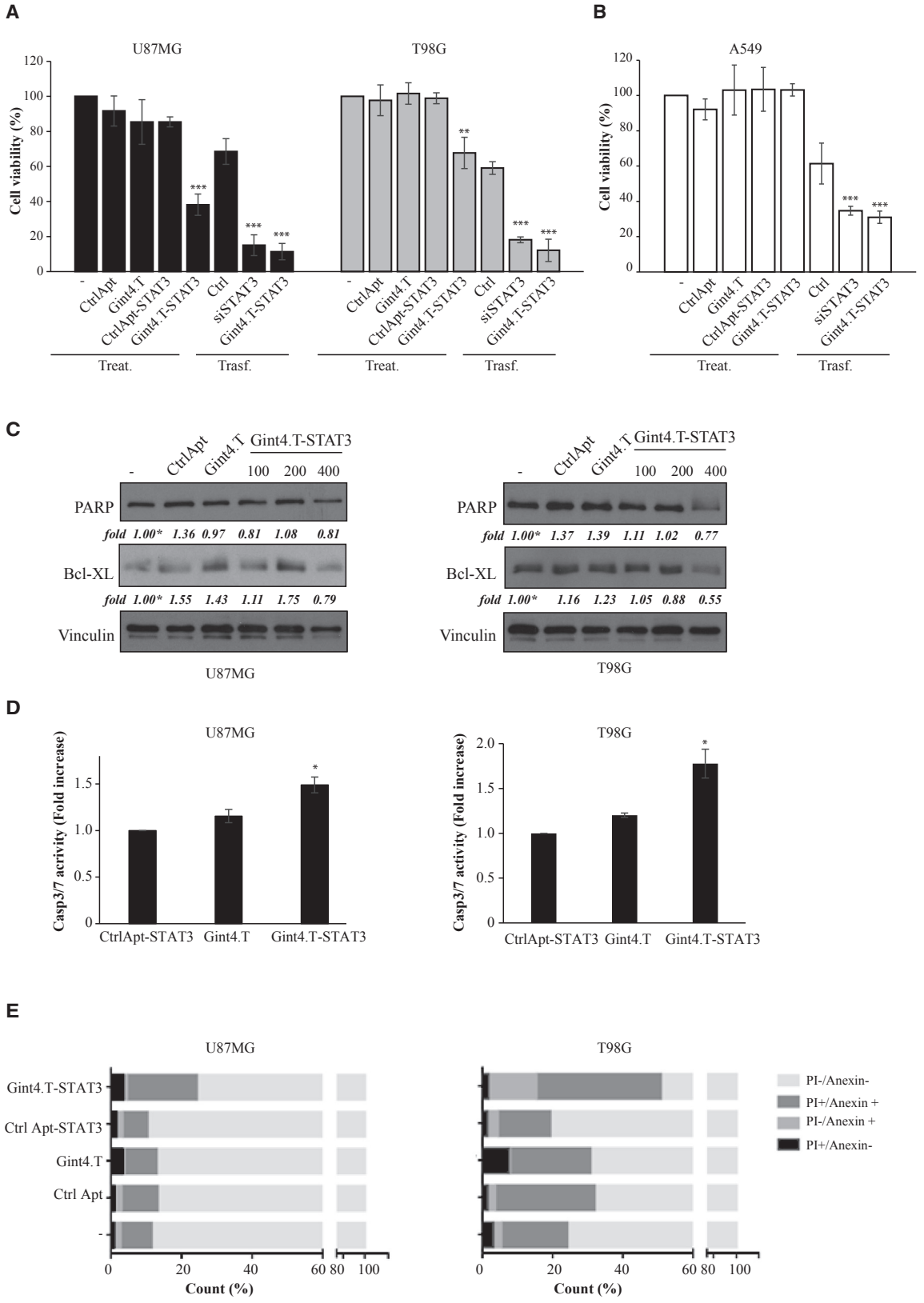

(legend on next page)

Gint4.T-STAT3 strongly reduces cell viability (Figure 2A). To confirm that inhibition was mediated by the aptamer-dependent recognition of the PDGFRβ, we analyzed by (3-(4,5-dimethylthiazol-2-yl)-2,5-diphenyltetrazolium bromide) (MTT) the effects of AsiC treatment on A549 cells that express low levels of PDGFRβ (Figure S2A). As shown in Figure 2B, the A549 cell viability was not affected by treatment with STAT3 AsiC but was instead strongly reduced upon transfection of either the AsiC or the siRNA moiety alone. Remarkably, no cytotoxicity was observed by treating the three cell lines with the unrelated control aptamer conjugated or not to STAT3 siRNA. These data indicate that the AsiC functionally regulates STAT3 in a receptor-dependent manner.

In order to further investigate the molecular mechanism that reduces cell viability, we monitored the expression of apoptosis markers following AsiC treatments in PDGFRβ-expressing cell lines. We analyzed the levels of full-length Poly (ADP-ribose) polymerase (PARP), whose activation by cleavage is involved in cell death, and of Bcl-XL, a downstream target of STAT3 that negatively regulates the apoptosis. We found that the AsiC reduces the levels of PARP and Bcl-XL proteins in both U87MG and T98G cells (Figure 2C). These data correlate with the increase of caspase-3/7 activity upon AsiC treatment (Figure 2D). Accordingly, as assessed by flow cytometry, Gint4.T-STAT3 determines an increase in the percent of double-labeled Annexin V/propidium iodide $(PI)^+$ cells (Figure 2E), suggesting that Gint4.T-STAT3 treatment decreases cell survival by triggering programmed cell death. No changes in distribution of cell cycle phases were found upon STAT3 AsiC treatment (data not shown).

STAT3 activation has been reported to be implicated also in the regulation of cell migration and metastatic potential of cancers.[39,40] Thus, we next determined whether STAT3 AsiC could impair GBM cell migration. As shown in Figures 3A and 3B, treating T98G and U87MG cells with Gint4.T-STAT3 strongly reduced cell migration as compared with the control aptamer or conjugate, cooperating with Gint4.T moiety function to produce a synergistic effect on cell motility.[32] In accordance with the dependence of STAT3 AsiC functional activity from the aptamer recognition of the PDGFRβ, we found that the AsiC has no effects on A549 ($PDGFR\beta^-$) cell migration (Figure 3C). In addition, by wound-healing assay, we detected a significant delay of wound closure in the presence of Gint4.T-STAT3 AsiC treatment compared with control in both U87MG and T98G $PDGFR\beta^+$ cells (Figure 3D).

Collectively, these results suggest that upon AsiC treatment, STAT3 is selectively downregulated in PDGFRβ-expressing cells that, consequently, become less viable, undergo apoptosis, and show impairment in cell motility.

In Vivo Activity of Gint4.T-STAT3 AsiC

One of the key aspects for therapeutic RNA clinical translation is their resistance to enzymatic degradation. We thus evaluated serum stability of Gint4.T AsiC by incubating the conjugate in 80% human serum for increasing times. Serum-RNA samples were analyzed by nondenaturing PAGE. As shown in Figure 4A, we found that the conjugate possesses an acceptable serum stability, not being visibly degraded up to 24 hr and then starting to be gradually hydrolyzed (cleaved).

To assess the effect of Gint4.T STAT on tumor growth *in vivo*, we injected U87MG cells in athymic nude mice. Tumor-bearing mice were treated with Gint4.T aptamer or Gin4.T-STAT3 AsiC (1,600 pmol/injection, i.e. 0.5–1 mg/kg) by intraperitoneal administration basing on previously published AsiC *in vivo* study.[24] Tumor volumes were measured at various times. As shown (Figure 4B), treatment with Gint4.T-STAT3 induces a more significant reduction of tumor growth rate as compared to the Gint4.T aptamer alone. Twenty days after tumor cell implantation, mice were euthanized and tumor growth was evaluated by tumor weight and histopathology. A representative image of resected tumors highlights that the group of mice treated with Gint4.T-STAT3-developed tumors smaller in size than the control and Gint4.T-treated group (Figure 4C). Tumors from the Gint4.T-STAT3 group had a lower weight than those from control and Gint4.T, with a mean of 120 mg, compared to 550 mg and 300 mg of the two other groups, respectively ($n = 5$; $^*p < 0.05$) (Figure 4D).

The role of Gint4.T-STAT on tumor growth was further investigated by immunohistochemistry (IHC). As shown in Figure 4E, cellular density was significantly reduced in *xenografts* exposed to Gint4.T-STAT3 compared to Gint4.T ($p < 0.05$) (higher panels). Furthermore, the control *xenografts* showed the presence of extensive areas of cells positive for Ki67 (approximately 50%, lower panels), a nuclear antigen associated with tumor cell proliferation. Gint4.T slightly reduced the areas of $Ki67^+$ cells relative to control. In contrast, in tumors from the Gint4.T-STAT3-treated group, $Ki67^+$ cells was reduced to approximately 25%.

Next, we determined by qRT-PCR the expression levels in tumors derived from AsiC-treated mice of STAT3 and STAT3 downstream

Figure 2. Gint4.T-STAT3 Functional Effects on Cell Viability and Apoptosis

(A and B) Cell viability of U87MG, T98G ($PDGFR\beta^+$, A), or A549 ($PDGFR\beta^-$, B) cells treated (at 400 nmol/L concentration) or transfected (at 100 nmol/L concentration) for 72 hr as indicated, was measured and expressed as percent of viable cells with respect to untreated cells (–). Error bars depict mean ± SD. Ctrl, transfection control; Treat., treatment; Transf., transfection. (C) Cell lysates from U87MG or T98G cells treated for 96 hr with 400 nmol/L Gint4.T or control aptamer or with indicated concentration of Gint4.T-STAT3 were immunoblotted with anti-PARP, anti-Bcl-XL, and anti-vinculin (used as a loading control) antibodies. Values below the blots indicate quantization relative to untreated (–, labeled with asterisk) normalized on the loading control signals. (D) The Caspase 3/7 activation was measured by Caspase-Glo 3/7 assay following 96 hr of U87MG or T98G cell treatment with 400 nmol/L of Gint4.T, Gint4.T-STAT3 AsiC, or control conjugate (CtrlApt-STAT3). Bars show the mean ± SD values. (E) Annexin V/PI staining was analyzed by flow cytometry in U87MG or T98G treated with indicated aptamers or conjugates for 96 hr. In (A), (B), and (D), statistics were calculated using Student's t test, $^*p < 0.05$; $^{**}p < 0.01$; $^{***}p < 0.001$ (versus untreated).

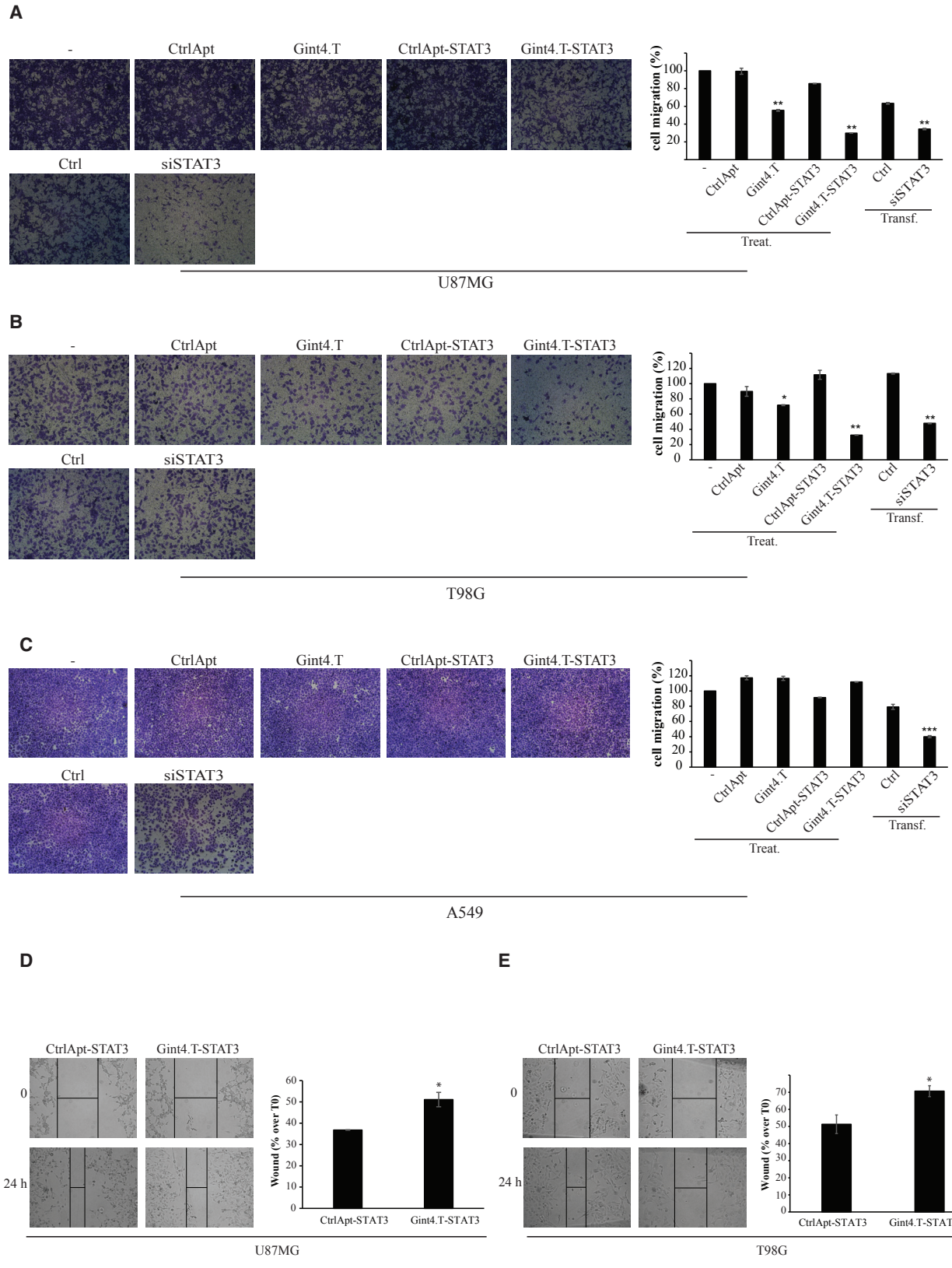

(legend on next page)

targets actively involved in cell growth and proliferation in many cancer types. As shown, treatment resulted in reduced levels of STAT3 (Figure 5A) and STAT3 target genes (cMyc, MCL-1, Bcl-2, HIF-1α, and Bcl-XL; Figure 5B),[41,42] probably as the consequence of reduced levels of phospho-STAT3 (Tyr 705) (Figure 5C).

In accordance with *in vitro* results (Figure 2), we also observed a reduction of pro-caspase 3, PARP, and Bcl-XL anti-apoptotic protein levels in tumor masses from mice treated with Gint4.T-STAT3, indicating the activation of the apoptotic process (Figure 5C). In addition, we analyzed the levels of Programmed cell death ligand 1 (PDL1) whose upregulation on tumor cells has been found to correlate JAK/STAT3 oncogenic signaling and play a crucial role in the immune escape in several cancers, including gliomas.[43] As shown (Figure 5D), Gint4.T-STAT3-treated tumors showed reduced levels of PDL1 mRNA and protein as compared to Gint4.T-treated or untreated samples, suggesting the potential development of the STAT3 AsiC as an immune-sensitizing approach for GBM.

Because GBM are highly vascularized tumors, we also studied the ability of tumor cells to transdifferentiate into endothelial cells *in vivo* by measuring the relative amount of vessels of human origin. Tumor sections stained with human CD31 antibody that marks mature vessels detected several vascularized areas in control group mice (n = 5) particularly evident at 200× magnification. Sections from Gint.4T-treated mice showed a decrease (2-fold lower than untreated mice) of vessels number that appear as strong brown circles. Gint4.T-STAT3 group showed a number of vessel comparable to Gint.4T control group (40 ± 10 vessels/section versus 30 ± 8 vessels/section), although the CD31 staining was very faint, suggesting the presence of immature vessels (Figure 5E). Indeed, the largest difference among tumor vascularization was observed with Wilms' tumor gene 1 (WT1) antibody able to detect early and immature vessels (neoangiogenesis).[44] Sections from Gint4.T-STAT3-treated tumors were stained with WT1 antibody at 3-fold lower intensity than controls (Figures 5E and 5F). These data indicate that human tumor cells support or at least contribute to neoangiogenesis of *xenografts* and Gint4.T-STAT3 treatment reduced both tumor cells proliferation and neovascularization.

DISCUSSION

In the present study, we addressed STAT3 gene silencing by aptamer-siRNA chimera to selectively target GBM.[45] In order to drive the siRNA to GBM tumors, we used an aptamer (Gint4.T) that binds and inhibits the PDGFRβ, a receptor tyrosine kinase (RTK) frequently overexpressed in GBM and implicated in neovascularization.[46–48] A number of aptamers for transmembrane receptors have been previously reported to be effective targeting moieties of AsiC.[49] Accordingly, we have recently developed the Gint4.T aptamer for the specific delivery of miRNAs and miRNA inhibitors to GBM cells.[33,36] Further, by using an *ex vivo* tri-culture model, we have shown that Gint4.T either alone or conjugated was able to cross the blood-brain barrier (BBB) likely by using a receptor-mediated mechanism.[33]

In this study, the Gint4.T aptamer was conjugated to a siRNA specifically targeting STAT3[30] to generate a fully modified 2′F-Py nuclease-resistant RNA conjugate. Our results demonstrated that upon AsiC treatment, STAT3 gene is silenced as assessed by the downregulation of STAT3 mRNA levels and by the consistent reduction of pY(705)-activated STAT3 protein (Figure 1). Yet, we found that upon the AsiC treatment, total STAT3 protein levels are less drastically reduced, as compared to the pY(705)-STAT3, suggesting the presence of a more stable fraction in the protein pool. Indeed, this is also indicated by the observation that upon CHX treatment, only a portion of STAT3 is rapidly degraded, while a fraction remains quite stable, with 30% of total protein levels lasting for several hours. However, the STAT3 fraction that is not phosphorylated in Y(705) looks to be poorly implicated in promoting cell growth and migration that are instead well inhibited by the AsiC treatment (Figures 2 and 3). Notably, STAT3-specific siRNA transfection inhibits cell viability and migration irrespective of the PDGFRβ expression, whereas treatments with Gint4.T AsiC lead to selective functional effects only on cells that express high levels of the PDGFRβ.

Furthermore, as we previously reported, the unconjugated Gint4.T aptamer inhibiting the target PDGFRβ activity is able to reduce by its own cell migration and tumor growth.[32] Here, we show that the Gint4.T AsiC effectively hampers *in vitro* cell migration, further enhancing the functional effect of the Gint4.T aptamer moiety. Most importantly, we addressed the *in vivo* potential of the AsiC by using, as a model, mice with tumor *xenograft* from U87MG cells. The systemic *in vivo* treatments with the AsiC leads to the drastic inhibition of tumor burden that results from the combination in the chimera of the PDGFRβ inhibition by Gint4.T with the STAT3 downregulation by the siRNA (Figure 4). On the other hand, GBM is an infiltrative tumor characterized by intense vascularization. We therefore also addressed the intra-tumor vascular response to AsiC administration and show that treatments are able to reduce the presence of human CD31- and WT1-expressing cells (Figure 5), as an indication of the inhibition of neovascularization.[50] Since WT1 has been reported as key regulator of cancer growth by modulating tumor

Figure 3. Gint4.T-STAT3 Functional Effects on Cell Migration

(A–C) Cell motility of U87MG (A), T98G (PDGFRβ$^+$, B), or A549 (PDGFRβ$^-$, C) was analyzed following 24 hr of indicated treatments (Treat.) or transfections (Transf.). Left, representative microphotographs are shown. Right, results were quantified and expressed as percent of migrated with respect to untreated cells (–). Ctrl, transfection control. Vertical bars indicate the SD values. (D and E) Confluent monolayers of U87MG (D) or T98G (E) cells treated with Gint4.T-STAT3 AsiC or CtrlApt-STAT3 control chimera were subjected to scratch assay, and wound closure was measured after 24 hr. Left, phase-contrast microscopy images are shown. Right, the wound dimension was calculated and expressed relative to the starting time (T0). (A–E) Magnification 10×. Statistics were calculated using Student's t test, *p < 0.05; **p < 0.01; ***p < 0.001 (versus untreated).

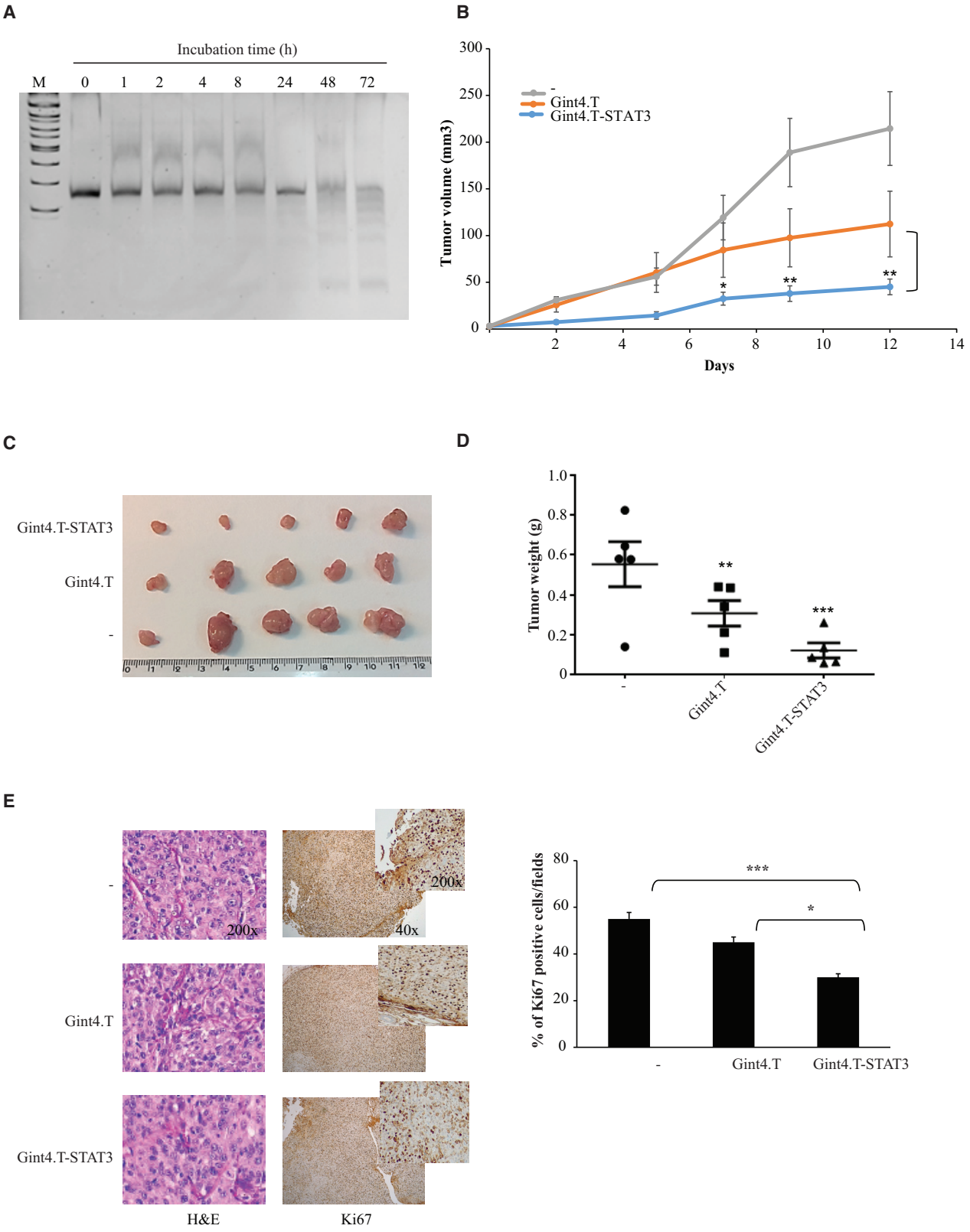

(legend on next page)

vascularization, immune response and metastasis formation in several cancer types,[44] the evidence that the AsiC conjugate is able to efficiently reduce WT1-expressing cells reinforces its potential as candidate for GBM treatment. In addition, we show that AsiC-treated tumors have reduced levels of the immune checkpoint protein PDL1, whose expression has been correlated with the activation of JAK/STAT3 oncogenic signaling.[51,52] Although a direct regulation by STAT3 in GBM has not yet been demonstrated, it has been shown that PDL1 expression is upregulated in high-grade GBM and associated with mesenchymal subtype markers.[53,54] By binding its target, the programmed cell death protein-1 (PD1), PDL1 plays a pivotal role in the escape of immune surveillance. Consequently, its targeting is reputed a highly promising therapeutic strategy for several cancer types including GBM. Therefore, the downregulation of PDL1 by the AsiC treatment, likely mediated through the STAT3 silencing, suggests a potential immunostimulatory application in GBM for the chimera.

Although the ability of the AsiC to successfully penetrate into intracranial models of GBM and functionally downregulate STAT3 to reduce tumor growth remains to be determined, recent evidence supports the ability of the targeting moiety, Gint4.T, to drive molecular carriers to the tumor site through the BBB.[33,55]

Taken together, our findings indicate that the STAT3 AsiC has the potential to selectively target cancer cells that overexpress the PDGFRβ and to interfere with multiple processes including cell survival, migration, and angiogenesis.

Collectively, our study represents a proof of principle for the development of a novel AsiC-based therapeutic to target GBM tumors.

MATERIALS AND METHODS

Aptamers and Conjugates

Gint4.T, 5′-UGUCGUGGGGCAUCGAGUAAAUGCAAUUCGACA-3′;

Gint4.T stick, 5′-UGUCGUGGGGCAUCGAGUAAAUGCAAUUCGACA*XXXX*GUACAUUCUAGAUAGCC-3′;

control aptamer (indicated as CtrlApt),

5′-UUCGUACCGGGUAGGUUGGCUUGCACAUAGAACGUGUCA-3′;

control aptamer stick (used in the control conjugate),

5′-GCCGCUAGAACCUUCUAAGCGAAUACAUUACCGC*XXXX*GUACAUUCUAGAUAGCC-3′;

human STAT3 antisense strand stick (STAT3 antisense [AS]-stick),

5′-UUAGCCCAUGUGAUCUGACACCCUGAAGGCUAUCUAGAAUGUAC-3′;

human STAT3 sense strand (STAT3 SS), 5′-CAGGGUGUCAGAUCACAUGGGCUAA-3′

All RNA sequences were purchased from Tebu-bio srl (Magenta, Milan, Italy) and contained 2′-F-Pyrimidines (2′-F-Py). Stick sequences consisting of 2′-F-Py and 2′-oxygen-methyl purines is underlined. The italic X indicates a three-carbon linker ((CH2)3) spacer. Before each treatment, aptamers were subjected to a short denaturation-renaturation step by incubating 5 min at 85°C, 3 min on ice, 10 min at 37°C. To prepare Gint4.T or control conjugates, STAT3 AS stick and STAT3 SS were annealed by incubating in annealing buffer (20 mM 2-[4-(2- hydroxyethyl)piperazin-1-yl] ethane sulfonic acid [HEPES; pH 7.5], 150 mM NaCl, 2 mM CaCl2) at 95°C for 10 min, 55°C for 10 min, and then at 37°C for 20 min. The AS-SS duplex was then incubated with refolded stick aptamer at 37°C for 30 min. The annealing was evaluated as the appearance of a shifted band on a 12% non-denaturing polyacrylamide gel.

Cells and Transfection

Human glioma U87MG and T98G cells or NSCLC A549 cells were provided by ATCC (American Type Culture Collection, Manassas, VA). Growth media used were as follows: DMEM (Sigma-Aldrich, St. Louis, MO, USA) for U87MG and T98G cells and RPMI (Sigma-Aldrich, St. Louis, MO, USA) for A549, both supplemented with 10% fetal bovine serum (FBS) (Sigma-Aldrich, St. Louis, MO, USA).

Transfections were performed using serum-free Opti-MEM and Lipofectamine 2000 reagent (Invitrogen, Waltham, MA, USA) according to the manufacturer's protocol. Cells were transfected with 100 nmol/L (where indicated) of annealed STAT3 siRNA (duplex of STAT3 AS-stick-STAT3 SS) or conjugate.

Figure 4. Gint4.T-STAT3 Serum Stability and Efficacy on Tumor Growth Inhibition

(A) Serum stability of Gint4.T-STAT3 AsiC (see Materials and Methods for details). (B–D) NOD/SCID nude mice bearing U87MG (PDGFRβ$^+$) were injected intraperitoneally with PBS (–) or 1,600 pmol of Gint4.T or Gint4.T-STAT3 AsiC (on days 0, 2, 5, 7, and 9). Mice were scarified at day 12 for further analyses. (B) Tumor volumes were measured by caliper and experimental raw data were interpolated with curve fitting or regression analysis. Error bars depict mean ± SEM (n = 10). Day 0 marks the start of treatments. Statistics calculated using two-way ANOVA versus Gint4.T are shown, *$p < 0.05$; **$p < 0.01$. Statistics versus untreated are as follows: Gint4.T-STAT3, $p < 0.001$ at days 7, 9, and 12; Gint4.T, $p < 0.001$ at days 9 and 12. (C) Representative picture of tumors (n = 5) recovered at the end of the *in vivo* experiment. (D) Weight of tumors (n = 5) recovered at the end of the *in vivo* experiment. Mean values ± SEM are indicated. One-way ANOVA was applied for statistics, **$p < 0.01$; ***$p < 0.001$. (E) Left, H&E and Ki67 staining of mice tumors treated with PBS, Gint4.T, or Gint4.T-STAT3 AsiC as reported in Figure 3. Magnifications are indicated. Right, plot reporting percentage of Ki67$^+$ cells/field. Data report the mean value of Ki67 staining per field in four fields scored per section (n = 5 per group). Statistics performed with Student's t test are indicated, *$p < 0.05$, ***$p < 0.001$.

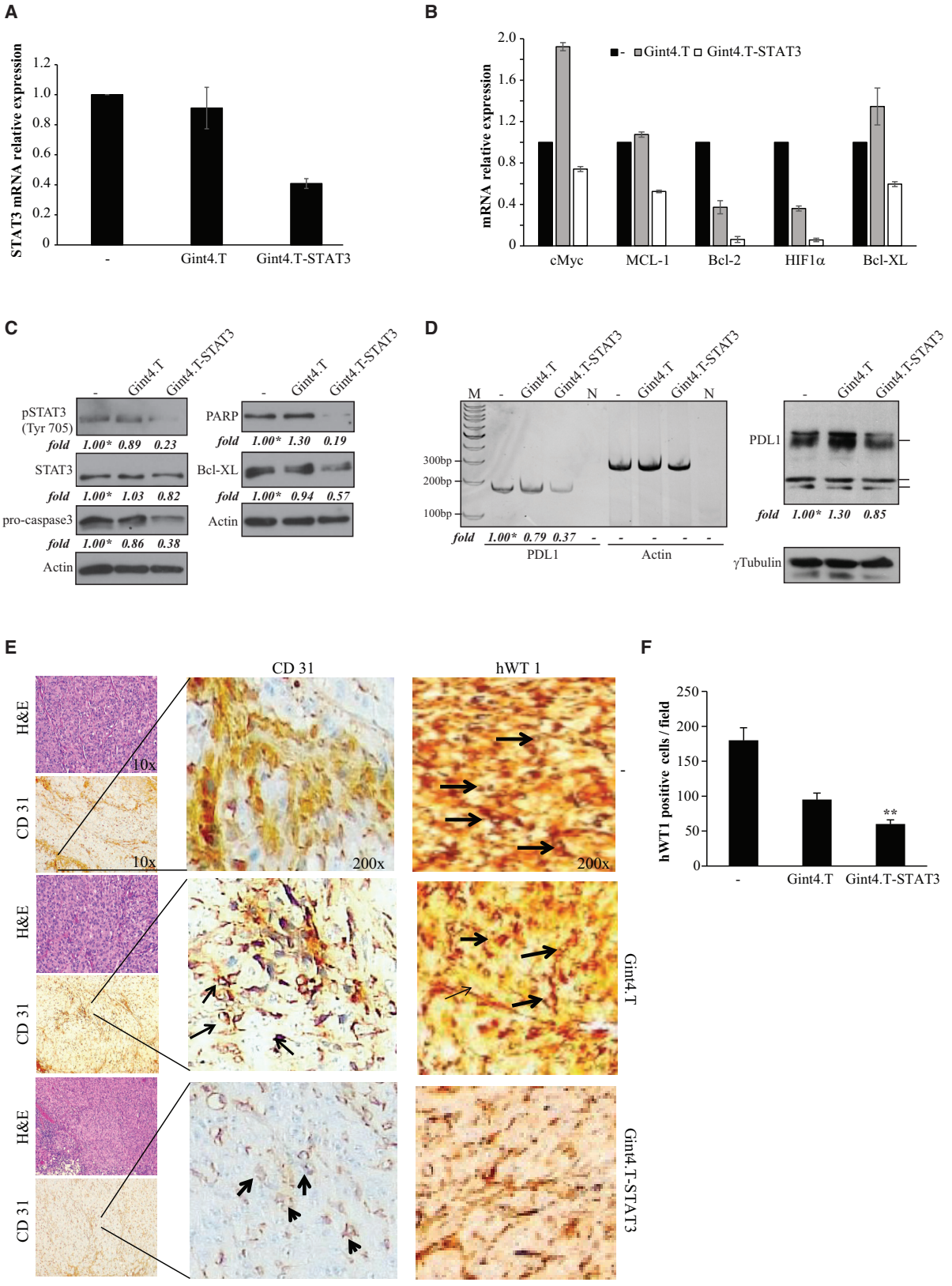

(legend on next page)

Immunoblot and RT-PCR Analysis

The day before conjugate treatment or transfection, cells were seeded in 3.5-cm plates (1×10^5 cells/plate). For CHX treatment, T98G cells were seeded in 6-well plates ($1.4 \times\times 10^5$ cells/well) and treated with 10 μg/mL CHX (Sigma, St. Louis, MO) from 0 to 24 hr.

Cell lysates were prepared in JS buffer (50 mM HEPES [pH 7.5], 50 mM NaCl, 1% glycerol, 1% Triton X-100, 1.5 mM $MgCl_2$, 5mM EGTA, 1 mM Na3VO4, protease inhibitors), boiled in sodium dodecyl sulfate/β-mercaptoethanol sample buffer, and separated by electrophoresis. Gels were blotted onto polyvinylidene difluoride membranes (Millipore, Billerica, MA, USA) and subjected to immunoblotting. Primary antibodies used were as follows: anti-PDGFRβ, anti-pY(705)-STAT3, pS(727)-STAT3, anti-STAT3, anti-PARP, anti-BCL-XL, anti-caspase3, p53, anti-Vinculina (Cell Signaling Technology Inc., Danvers, MA, USA); anti-α-tubulin, anti-actin (Santa Cruz Biotechnology, CA, USA); anti-PDL1 (Novus Biologicals, Littleton, CO, USA).

RNAs were extracted with TRiZol (Invitrogen, Waltham, MA, USA). To analyze gene mRNA level, 1 μg of total RNA was reverse transcribed with iScript cDNA Synthesis Kit. For real-time PCR, amplification was performed with IQ-SYBR Green supermix (Bio-Rad, Hercules, CA, USA). Relative mRNA quantization was analyzed by using the ΔΔCt method applying the equation $2^{-\Delta\Delta Ct}$. PCR amplification of PDL1 was made with FIREPol DNA Polymerase (Microtech, Naples, Italy). PCR products were loaded on 10% non-denaturing polyacrylamide gel and visualized by UV exposure after ethidium bromide staining.

The specific primers used were as follows: STAT3 Fw, 5′-ACC TGCAGCAATACCATTGAC-3′; STAT3 Rev, 5′-AAGGTGAGGG ACTCAAACTGC-3′; β-actin Fw, 5′-CAAGAGATGGCCACGGCT GCT-3′; β-actin Rev, 5′-TCCTTCTGCATCCTGTCGGCA-3′; Myc Fw, 5′-GTCAAGAGGCGAACACACAAC-3′; Myc Rev, 5′-TTGG ACGGACAGGATGTATGC-3′; MCL-1 Fw, 5′-TGCTTCGGAAA CTGGACATCA-3′; MCL-1 Rev, 5′-TAGCCACAAAGGCAC CAAAAG-3′; Bcl-2 Fw, 5′-GGTGGGGTCATGTGTGTGG-3′; Bcl-2 Rev, 5′-CGGTTCAGGTACTCAGTCATCC-3′; Bcl-XL Fw, 5′-GAGC TGGTGGTTGACTTTCTC-3′; Bcl-XL Rev, 5′-TCCATCTCCGATT CAGTCCCT-3′; HIF-1α Fw, 5′-CATCTCCATCTCCTACCCACA-3′; HIF-1α Rev, 5′-CTTTTCCTGCTCTGTTTGGTG-3′; PDL1 Fw, 5′-GCTTTTCAATGTGACCAGCA-3′; PDL1 Rev, 5′-TGGCTCC CAGAATTACCAAG-3′.

Cell Viability and Caspase Assay

Cells were seeded in 96-well plates (2×10^3 cells/well) and left untreated, transfected, treated with aptamers, or conjugated, as indicated. CellTiter 96 Proliferation Assay (Promega, Madison, WI) was used to analyze cell viability. Caspase-Glo 3/7 luminescent Assay (Promega, Madison, WI) was used to measure caspase-3 and -7 activities, according to the manufacturer's instructions.

Flow Cytometry Analysis

For the Annexin V-fluorescein isothiocyanate (FITC)/PI apoptosis flow cytometry detection assay, cells were seeded in 3.5-cm plates (1×10^5 cells/plate) and treated with aptamers or chimeras (400 nmol/L). Cells were centrifuged for 5 min, washed twice with 1 mL of cold 1× PBS and then suspended in 1× binding buffer (1×10^6 cells/mL). Annexin V-FITC/PI staining was performed by using Annexin V apoptosis kit (Novus Biologicals, Littleton, CO, USA) following manufacturer's recommendations. Flow cytometry analysis was performed with BD Accuri C6 (BD Biosciences, Franklin Lakes, New Jersey, USA).

Transwell Migration and Wound-Healing Assays

For Transwell migration assay, cells were seeded in 3.5-cm plates (1.4×10^5 cells/plate) and transfected or treated with aptamers or chimeras (400 nmol/L), as indicated. After 24 hr, 1×10^5 cells were plated into the upper chamber of a 24-well transwell (Corning Incorporate, Corning, NY) in serum-free DMEM and exposed to 10% FBS as inducers of migration (0.6 mL, lower chamber) for an additional 24 hr. Staining with 0.1% crystal violet in 25% methanol was performed to visualize migrated cells, and pictures were acquired with Leica Application Suite. To quantify the percentage of migrated cells, crystal violet was evaluated with 1% sodium dodecyl sulfate, and the absorbance at 594 nm wavelength was measured.

For wound-healing assay, cells were plated in six-well plates and grown to confluence. Cells were serum starved overnight in the absence or in the presence of 400 nmol/L Gint4.T-STAT3 or the control conjugate and then scraped to induce a wound.

Figure 5. Gint4.T-STAT3 *In Vivo* Analyses

(A and D) Tumor masses from NOD/SCID nude mice bearing U87MG (PDGFRβ$^+$) treated with PBS (–), Gint4.T, or Gint4.T-STAT3 AsiC as reported in Figure 3 were processed for RNA or protein extraction. (A and B) The levels of STAT3, indicated STAT3 downstream target genes, or Actin (used for normalization) mRNA were measured by qRT-PCR in pooled RNAs. Vertical bars indicate SD on experimental replicates. (C) Immunoblot with anti-pY(705)-STAT3, anti-STAT3, anti-caspase3, anti-PARP, anti-Bcl-XL, and anti-actin (used as a loading control) antibodies of pooled lysates. (D) Left, PDL1 or Actin (used for normalization) mRNA levels were analyzed in pooled RNAs by RT-PCR. Samples from 40 PCR cycles were loaded on non-denaturing polyacrylamide gel. M, 100-bp molecular markers; N, PCR$^-$ controls. Values below the gel indicate quantization relative to untreated (–, labeled with asterisk) normalized on Actin signals. Right, immunoblot with anti-PDL1 and anti-γ-tubulin (used as a loading control) antibodies of pooled lysates. (C and D) Right, values below the blots indicate quantization relative to untreated (–, labeled with asterisk) normalized on the loading control signals. (E) Representative staining with CD31 and WT1 antibody in PBS-, Gint4.T-, or Gint4.T-STAT3-treated tumors. Magnification is indicated. Black arrows highlight vessels. (F) Graph reporting WT1$^+$ cells/field. Data report the mean value of four fields scored per section (n = 5). Statistical analyses were performed with Student's t test: **$p < 0.01$ (versus PBS-treated mice).

Culture medium with 1% FBS with/without treatments was added, and the wounds were observed using phase-contrast microscopy.

Stability in Human Serum

Gint4.T-STAT3 conjugates were incubated at 4 μM in 80% human serum (Type AB Human Serum provided by Euroclone) for increasing time points (from 1 hr to 72 hr). At each time point, 4 μL (16 pmoles RNA) was recovered and incubated for 1 hr at 37°C with 0.5 μL of proteinase K solution (600 mAU/mL) in order to remove serum proteins. Then, 4.5 μL 1 × Tris-borate-EDTA (TBE) and 1 μL gel loading buffer (Invitrogen, Waltham, MA, USA) were added to each sample before storing at −80°C. All time point samples were loaded on 10% non-denaturing polyacrylamide gel. The gel was visualized by UV exposure after ethidium bromide staining.

In Vivo Animal Study

U87MG cells (5×10^6/mouse) were injected subcutaneously into two flanks of 6- to 8-week-old NOD/SCID nude mice (Charles River). After 7 days, mice were divided into three groups of five. One group received intra-peritoneal injections of Gint4.T-STAT (1,600 pmoles/injection/mouse in 100 μL/injection). The other control groups received PBS and Gint4.T (1,600 pmoles/injection/mouse in 100 μL/injection), respectively, allowed by local Ethics Committee guidelines. Tumor size was determined by microcallipers and calculated according to the following formula: tumor volume (mm^3) = $L \times W^2/2$, where L is the length and W is the width. After 12 days from the starting of the treatment, the mice were sacrificed by CO_2 asphyxiation. Tumors were excised, weighed, lysed for RNA/protein extraction, or stored in 10% paraffin for following IHC. For histological examinations, sections of 4–5μm of tumors were deparaffinized and stained with H&E and then with CD31 (JC/70) and WT1 (6F/H2 Ventana Medical Systems) and Ki67 (Dako). All the antibodies were used at dilution 1:100. The sections were then stained using avidin-biotin complex by immunoperoxidase technique. Labeling index and number of the total of nuclei in each field were scored, and the ratio of two values was calculated by Image-Pro Plus 6.0 software automatically under Leica microscope.

The animal experiments were approved by the Animal Ethics Committee of the Italian Ministry of Health (764/2016-PR).

Statistical Analyses

Statistical analyses were performed by t test or ANOVA with GraphPad Prism v.6.0, as indicated.

SUPPLEMENTAL INFORMATION

Supplemental Information includes Supplemental Materials and Methods and two figures and can be found with this article online at https://doi.org/10.1016/j.omtn.2017.12.021.

AUTHOR CONTRIBUTIONS

C.L.E. designed and performed the majority of the experiments, interpreted results, and assisted with manuscript preparation. S.N., S.C., and S.R. performed and/or assisted with several experiments. F.d.N. performed and contributed to interpreting the *in vivo* experiments. V.d.F. provided intellectual input, coordinated the research, secured the funding, and guided result interpretation and manuscript preparation.

CONFLICTS OF INTEREST

The authors declare no conflict of interest.

ACKNOWLEDGMENTS

We wish to thank M.F. Romano, P.H. Giangrande, and G. Condorelli for suggestions and L. Baraldi and F. Moscato for technical assistance. This work was supported by funds from the AIRC (13345 and 9980; V.d.F.), the CNR Flagship Project NanoMax (DESIRED; V.d.F.), and the Italian Ministry of Health (GR-2011-02352546; C.L.E.).

REFERENCES

1. Louis, D.N., Perry, A., Reifenberger, G., von Deimling, A., Figarella-Branger, D., Cavenee, W.K., Ohgaki, H., Wiestler, O.D., Kleihues, P., and Ellison, D.W. (2016). The 2016 World Health Organization classification of tumors of the central nervous system: a summary. Acta Neuropathol. *131*, 803–820.

2. Louis, D.N., Perry, A., Burger, P., Ellison, D.W., Reifenberger, G., von Deimling, A., Aldape, K., Brat, D., Collins, V.P., Eberhart, C., et al.; International Society of Neuropathology—Haarlem (2014). International Society of Neuropathology—Haarlem consensus guidelines for nervous system tumor classification and grading. Brain Pathol. *24*, 429–435.

3. Kwiatkowska, A., and Symons, M. (2013). Signaling determinants of glioma cell invasion. Adv. Exp. Med. Biol. *986*, 121–141.

4. Fortin Ensign, S.P., Mathews, I.T., Symons, M.H., Berens, M.E., and Tran, N.L. (2013). Implications of Rho GTPase signaling in glioma cell invasion and tumor progression. Front. Oncol. *3*, 241.

5. Katsetos, C.D., Dráberová, E., Smejkalová, B., Reddy, G., Bertrand, L., de Chadarévian, J.P., Legido, A., Nissanov, J., Baas, P.W., and Dráber, P. (2007). Class III beta-tubulin and gamma-tubulin are co-expressed and form complexes in human glioblastoma cells. Neurochem. Res. *32*, 1387–1398.

6. Han, T.J., Cho, B.J., Choi, E.J., Kim, D.H., Song, S.H., Paek, S.H., and Kim, I.A. (2016). Inhibition of STAT3 enhances the radiosensitizing effect of temozolomide in glioblastoma cells in vitro and in vivo. J. Neurooncol. *130*, 89–98.

7. Fan, Q.W., Cheng, C.K., Gustafson, W.C., Charron, E., Zipper, P., Wong, R.A., Chen, J., Lau, J., Knobbe-Thomsen, C., Weller, M., et al. (2013). EGFR phosphorylates tumor-derived EGFRvIII driving STAT3/5 and progression in glioblastoma. Cancer Cell *24*, 438–449.

8. Carro, M.S., Lim, W.K., Alvarez, M.J., Bollo, R.J., Zhao, X., Snyder, E.Y., Sulman, E.P., Anne, S.L., Doetsch, F., Colman, H., et al. (2010). The transcriptional network for mesenchymal transformation of brain tumours. Nature *463*, 318–325.

9. Kim, E., Kim, M., Woo, D.H., Shin, Y., Shin, J., Chang, N., Oh, Y.T., Kim, H., Rheey, J., Nakano, I., et al. (2013). Phosphorylation of EZH2 activates STAT3 signaling via STAT3 methylation and promotes tumorigenicity of glioblastoma stem-like cells. Cancer Cell *23*, 839–852.

10. Sherry, M.M., Reeves, A., Wu, J.K., and Cochran, B.H. (2009). STAT3 is required for proliferation and maintenance of multipotency in glioblastoma stem cells. Stem Cells *27*, 2383–2392.

11. Xiong, A., Yang, Z., Shen, Y., Zhou, J., and Shen, Q. (2014). Transcription factor STAT3 as a novel molecular target for cancer prevention. Cancers (Basel) *6*, 926–957.

12. Wang, T., Niu, G., Kortylewski, M., Burdelya, L., Shain, K., Zhang, S., Bhattacharya, R., Gabrilovich, D., Heller, R., Coppola, D., et al. (2004). Regulation of the innate

and adaptive immune responses by Stat-3 signaling in tumor cells. Nat. Med. *10*, 48–54.

13. Yu, H., Lee, H., Herrmann, A., Buettner, R., and Jove, R. (2014). Revisiting STAT3 signalling in cancer: new and unexpected biological functions. Nat. Rev. Cancer *14*, 736–746.

14. Jackson, C., Ruzevick, J., Amin, A.G., and Lim, M. (2012). Potential role for STAT3 inhibitors in glioblastoma. Neurosurg. Clin. N. Am. *23*, 379–389.

15. Luwor, R.B., Stylli, S.S., and Kaye, A.H. (2013). The role of Stat3 in glioblastoma multiforme. J. Clin. Neurosci. *20*, 907–911.

16. Furtek, S.L., Backos, D.S., Matheson, C.J., and Reigan, P. (2016). Strategies and approaches of targeting STAT3 for cancer treatment. ACS Chem. Biol. *11*, 308–318.

17. Wake, M.S., and Watson, C.J. (2015). STAT3 the oncogene—still eluding therapy? FEBS J. *282*, 2600–2611.

18. Zhang, Q., Hossain, D.M., Duttagupta, P., Moreira, D., Zhao, X., Won, H., Buettner, R., Nechaev, S., Majka, M., Zhang, B., et al. (2016). Serum-resistant CpG-STAT3 decoy for targeting survival and immune checkpoint signaling in acute myeloid leukemia. Blood *127*, 1687–1700.

19. Kortylewski, M., and Nechaev, S. (2014). Cancer therapy using oligonucleotide-based STAT3 inhibitors: will they deliver? Ther. Deliv. *5*, 239–242.

20. Barar, J., Rafi, M.A., Pourseif, M.M., and Omidi, Y. (2016). Blood-brain barrier transport machineries and targeted therapy of brain diseases. Bioimpacts *6*, 225–248.

21. Keefe, A.D., Pai, S., and Ellington, A. (2010). Aptamers as therapeutics. Nat. Rev. Drug Discov. *9*, 537–550.

22. Catuogno, S., and Esposito, C.L. (2017). Aptamer cell-based selection: overview and advances. Biomedicines *5*, E49.

23. Catuogno, S., Esposito, C.L., and de Franciscis, V. (2016). Aptamer-mediated targeted delivery of therapeutics: an update. Pharmaceuticals (Basel) *9*, E69.

24. Dassie, J.P., Liu, X.Y., Thomas, G.S., Whitaker, R.M., Thiel, K.W., Stockdale, K.R., Meyerholz, D.K., McCaffrey, A.P., McNamara, J.O., 2nd, and Giangrande, P.H. (2009). Systemic administration of optimized aptamer-siRNA chimeras promotes regression of PSMA-expressing tumors. Nat. Biotechnol. *27*, 839–849.

25. Gilboa-Geffen, A., Hamar, P., Le, M.T., Wheeler, L.A., Trifonova, R., Petrocca, F., Wittrup, A., and Lieberman, J. (2015). Gene knockdown by EpCAM aptamer-siRNA chimeras suppresses epithelial breast cancers and their tumor-initiating cells. Mol. Cancer Ther. *14*, 2279–2291.

26. Neff, C.P., Zhou, J., Remling, L., Kuruvilla, J., Zhang, J., Li, H., Smith, D.D., Swiderski, P., Rossi, J.J., and Akkina, R. (2011). An aptamer-siRNA chimera suppresses HIV-1 viral loads and protects from helper CD4(+) T cell decline in humanized mice. Sci. Transl. Med. *3*, 66ra6.

27. Wheeler, L.A., Trifonova, R., Vrbanac, V., Basar, E., McKernan, S., Xu, Z., Seung, E., Deruaz, M., Dudek, T., Einarsson, J.I., et al. (2011). Inhibition of HIV transmission in human cervicovaginal explants and humanized mice using CD4 aptamer-siRNA chimeras. J. Clin. Invest. *121*, 2401–2412.

28. Wheeler, L.A., Vrbanac, V., Trifonova, R., Brehm, M.A., Gilboa-Geffen, A., Tanno, S., Greiner, D.L., Luster, A.D., Tager, A.M., and Lieberman, J. (2013). Durable knockdown and protection from HIV transmission in humanized mice treated with gel-formulated CD4 aptamer-siRNA chimeras. Mol. Ther. *21*, 1378–1389.

29. Zhou, J., Li, H., Zhang, J., Piotr, S., and Rossi, J. (2011). Development of cell-type specific anti-HIV gp120 aptamers for siRNA delivery. J. Vis. Exp. *52*, 2954.

30. Herrmann, A., Priceman, S.J., Swiderski, P., Kujawski, M., Xin, H., Cherryholmes, G.A., Zhang, W., Zhang, C., Lahtz, C., Kowolik, C., et al. (2015). CTLA4 aptamer delivers STAT3 siRNA to tumor-associated and malignant T cells. J. Clin. Invest. *125*, 2547.

31. Zhou, J., Rossi, J.J., and Shum, K.T. (2015). Methods for assembling B-cell lymphoma specific and internalizing aptamer-siRNA nanoparticles via the sticky bridge. Methods Mol. Biol. *1297*, 169–185.

32. Camorani, S., Esposito, C.L., Rienzo, A., Catuogno, S., Iaboni, M., Condorelli, G., de Franciscis, V., and Cerchia, L. (2014). Inhibition of receptor signaling and of glioblastoma-derived tumor growth by a novel PDGFRβ aptamer. Mol. Ther. *22*, 828–841.

33. Esposito, C.L., Nuzzo, S., Kumar, S.A., Rienzo, A., Lawrence, C.L., Pallini, R., Shaw, L., Alder, J.E., Ricci-Vitiani, L., Catuogno, S., and de Franciscis, V. (2016). A combined microRNA-based targeted therapeutic approach to eradicate glioblastoma stem-like cells. J. Control. Release *238*, 43–57.

34. Zhou, J., Neff, C.P., Swiderski, P., Li, H., Smith, D.D., Aboellail, T., Remling-Mulder, L., Akkina, R., and Rossi, J.J. (2013). Functional in vivo delivery of multiplexed anti-HIV-1 siRNAs via a chemically synthesized aptamer with a sticky bridge. Mol. Ther. *21*, 192–200.

35. Esposito, C.L., Cerchia, L., Catuogno, S., De Vita, G., Dassie, J.P., Santamaria, G., Swiderski, P., Condorelli, G., Giangrande, P.H., and de Franciscis, V. (2014). Multifunctional aptamer-miRNA conjugates for targeted cancer therapy. Mol. Ther. *22*, 1151–1163.

36. Catuogno, S., Rienzo, A., Di Vito, A., Esposito, C.L., and de Franciscis, V. (2015). Selective delivery of therapeutic single strand antimiRs by aptamer-based conjugates. J. Control. Release *210*, 147–159.

37. Reich, N.C., and Liu, L. (2006). Tracking STAT nuclear traffic. Nat. Rev. Immunol. *6*, 602–612.

38. Gkouveris, I., Nikitakis, N., and Sauk, J. (2015). STAT3 signaling in cancer. J. Cancer Ther. *6*, 709–726.

39. Carpenter, R.L., and Lo, H.W. (2014). STAT3 target genes relevant to human cancers. Cancers (Basel) *6*, 897–925.

40. Baskin, R., Park, S.O., Keserű, G.M., Bisht, K.S., Wamsley, H.L., and Sayeski, P.P. (2014). The Jak2 small molecule inhibitor, G6, reduces the tumorigenic potential of T98G glioblastoma cells in vitro and in vivo. PLoS ONE *9*, e105568.

41. Yao, S., Xu, F., Chen, Y., Ge, Y., Zhang, F., Huang, H., Li, L., Lin, D., Luo, X., Xu, J., et al. (2017). Fbw7 regulates apoptosis in activated B-cell like diffuse large B-cell lymphoma by targeting Stat3 for ubiquitylation and degradation. J. Exp. Clin. Cancer Res. *36*, 10.

42. Li, X., Liu, X., Xu, Y., Liu, J., Xie, M., Ni, W., and Chen, S. (2014). KLF5 promotes hypoxia-induced survival and inhibits apoptosis in non-small cell lung cancer cells via HIF-1α. Int. J. Oncol. *45*, 1507–1514.

43. Xue, S., Hu, M., Iyer, V., and Yu, J. (2017). Blocking the PD-1/PD-L1 pathway in glioma: a potential new treatment strategy. J. Hematol. Oncol. *10*, 81.

44. Wagner, K.D., Cherfils-Vicini, J., Hosen, N., Hohenstein, P., Gilson, E., Hastie, N.D., Michiels, J.F., and Wagner, N. (2014). The Wilms' tumour suppressor Wt1 is a major regulator of tumour angiogenesis and progression. Nat. Commun. *5*, 5852.

45. Bianco, J., Bastiancich, C., Jankovski, A., des Rieux, A., Préat, V., and Danhier, F. (2017). On glioblastoma and the search for a cure: where do we stand? Cell. Mol. Life Sci. *74*, 2451–2466.

46. Kim, Y., Kim, E., Wu, Q., Guryanova, O., Hitomi, M., Lathia, J.D., Serwanski, D., Sloan, A.E., Weil, R.J., Lee, J., et al. (2012). Platelet-derived growth factor receptors differentially inform intertumoral and intratumoral heterogeneity. Genes Dev. *26*, 1247–1262.

47. Nakada, M., Kita, D., Watanabe, T., Hayashi, Y., Teng, L., Pyko, I.V., and Hamada, J. (2011). Aberrant signaling pathways in glioma. Cancers (Basel) *3*, 3242–3278.

48. Akhavan, D., Pourzia, A.L., Nourian, A.A., Williams, K.J., Nathanson, D., Babic, I., Villa, G.R., Tanaka, K., Nael, A., Yang, H., et al. (2013). De-repression of PDGFRβ transcription promotes acquired resistance to EGFR tyrosine kinase inhibitors in glioblastoma patients. Cancer Discov. *3*, 534–547.

49. Kruspe, S., and Giangrande, P.H. (2017). Aptamer-siRNA chimeras: discovery, progress, and future prospects. Biomedicines *5*, E45.

50. Fazioli, F., Colella, G., Miceli, R., Di Salvatore, M.G., Gallo, M., Boccella, S., De Chiara, A., Ruosi, C., and de Nigris, F. (2017). Post-surgery fluids promote transition of cancer stem cell-to-endothelial and AKT/mTOR activity, contributing to relapse of giant cell tumors of bone. Oncotarget *8*, 85040–85053.

51. Abdelhamed, S., Ogura, K., Yokoyama, S., Saiki, I., and Hayakawa, Y. (2016). AKT-STAT3 pathway as a downstream target of EGFR signaling to regulate PD-L1 expression on NSCLC cells. J. Cancer *7*, 1579–1586.

52. Atsaves, V., Tsesmetzis, N., Chioureas, D., Kis, L., Leventaki, V., Drakos, E., Panaretakis, T., Grander, D., Medeiros, L.J., Young, K.H., and Rassidakis, G.Z. (2017). PD-L1 is commonly expressed and transcriptionally regulated by STAT3 and MYC in ALK-negative anaplastic large-cell lymphoma. Leukemia *31*, 1633–1637.

53. Heiland, D.H., Haaker, G., Delev, D., Mercas, B., Masalha, W., Heynckes, S., Gäbelein, A., Pfeifer, D., Carro, M.S., Weyerbrock, A., et al. (2017). Comprehensive analysis of PD-L1 expression in glioblastoma multiforme. Oncotarget *8*, 42214–42225.

54. Heynckes, S., Gaebelein, A., Haaker, G., Grauvogel, J., Franco, P., Mader, I., Carro, M.S., Prinz, M., Delev, D., Schnell, O., and Heiland, D.H. (2017). Expression differences of programmed death ligand 1 in de-novo and recurrent glioblastoma multiforme. Oncotarget *8*, 74170–74177.

55. Monaco, I., Camorani, S., Colecchia, D., Locatelli, E., Calandro, P., Oudin, A., Niclou, S., Arra, C., Chiariello, M., Cerchia, L., and Comes Franchini, M. (2017). Aptamer functionalization of nanosystems for glioblastoma targeting through the blood-brain barrier. J. Med. Chem. *60*, 4510–4516.